ROYAL SOCIETY OF CHEMISTRY

PAPER

Photo-triggerable hydrogel–nanoparticle hybrid scaffolds for remotely controlled drug delivery†

Shreyas Shah,‡ Pijus K. Sasmal‡ and Ki-Bum Lee*

Remotely-triggerable drug delivery systems enable the user to adjust dosing regimens on-demand based on a patient's physiological response and clinical needs. However, currently reported systems are limited by the non-specific leakage of drugs in the absence of triggering and the lack of repeatability over multiple cycles of release. To this end, we have designed a unique hydrogel–nanoparticle hybrid scaffold that provides a chemically-defined, remotely-triggerable and on-demand release of small molecule drugs. Our hybrid platform consists of three distinct components: (1) a photo-triggerable chemical compound, which serves to release a covalently-bound drug upon photo-irradiation, (2) a nanoparticle, which serves to covalently bind the photo-triggerable compound, and (3) a polymeric hydrogel, which serves to hold the drug-conjugated nanoparticle. Upon photo-irradiation, the activation of the photo-triggerable compound is designed to initiate a series of intramolecular chemical rearrangements, which would cleave the covalently-bound drug and release it from the hydrogel. The combination of these distinct components in a single scaffold proved to be an effective drug delivery system, as demonstrated by the delivery of a model drug to a malignant cancer line. Our hybrid scaffold can be easily tuned for practically any biological application of interest, thus offering immense potential for clinical therapies.

Introduction

Drug delivery systems are constantly advancing due to the importance of achieving targeted and controlled release. The current lack of control over the spatial and temporal administration of drugs tends to require larger doses in order to achieve the desired effect within the therapeutic window, which can inadvertently cause increased toxicity and other undesirable side effects.[1] Moreover, numerous drug treatment regimens require frequent or continuous administration based on the patient's response to the treatment over a period of time, which can compromise patient comfort and compliance. Addressing these concerns, recent advances in materials chemistry have led to the generation of reservoir-based drug delivery systems that release loaded drugs in response to an externally-applied stimulus.[2] Such systems allow for a highly localized concentration of drugs at or near the target site upon implantation, while enabling the patient or healthcare professional to control the dose and timing of drug release.[3]

Various types of remotely-triggerable drug delivery systems have been developed, which rely on applying an external stimuli to release the drug load.[4] One type of system employed a multi-

reservoir, microchip device which was triggered through a wirelessly transmitted signal.[5] Upon wireless triggering, the electrochemical dissolution of the drug-sealed membrane was shown to effectively release the drug. While such a device is effective for delivering multiple doses, the size of the solid-state device limits the implantation to only certain subcutaneous compartments in the body. Compared to these microfabricated solid-state devices, other systems have utilized soft materials (*e.g.* polymers) which undergo conformational changes due to microenvironmental conditions. For instance, thermo-responsive polymers or membranes consisting of drugs and gold nanoparticles (*i.e.* nanoshells, nanorods) have been shown to effectively release the embedded drug upon local heating of the gold nanoparticles *via* near infrared light irradiation.[6,7] In other variants of such a system, magnetic nanoparticles have been used in combination with an alternating magnetic field to impose local heating.[8,9] While local heat induction is one of the most widely investigated stimuli for such systems, the potential damage to healthy tissue from thermal injury and the possibility of accidental triggering (*e.g.* due to fever) can cause undesired side effects.[6]

In this regard, light can serve as a superior external stimulus for drug release since it can be manipulated to attain both spatial and temporal control with high precision.[10] In contrast to other types of remote triggers for drug delivery, light is the least invasive, it does not require advanced equipment, and the drug release can be modulated by simply adjusting the wavelength of light, power density and time of exposure.[11] Various

Department of Chemistry & Chemical Biology, Rutgers, The State University of New Jersey, Piscataway, NJ 08854, USA. E-mail: kblee@rutgers.edu; Fax: +1-732-445-5312; Tel: +1-848-445-2081

† Electronic supplementary information (ESI) available. See DOI: 10.1039/c4tb01436g

‡ These authors contributed equally to this work.

This journal is © The Royal Society of Chemistry 2014

J. Mater. Chem. B, 2014, **2**, 7685–7693 | 7685

types of photo-responsive drug carrier systems have been developed including prodrugs, micellar/liposomal vesicles, nanoparticles, self-immolative polymers and hydrogels.[12–15] Yet, there have been several challenges in creating effective photo-responsive reservoir-based systems which afford controlled release from a drug-embedded membrane or polymer matrix. Specifically, the majority of current approaches rely on simply encapsulating the drug or biomolecule of interest within a photodegradable polymer matrix (*e.g.* hydrogel), whereby the photo-induced degradation of the matrix releases the cargo.[16] However, such systems exhibit a poor ratio of drug release kinetics between the 'on' (light) and 'off' (no light) state. As a result, there is unintended leakage of drugs from the polymer reservoir in the absence of photo-irradiation due to passive diffusion, thus questioning the long-term stability and clinical-relevance of such systems. Moreover, such designs primarily allow for only one-time burst releases, compared to the favorable continuous or pulsatile release from multiple cycles of photo-irradiation over a given time frame. Considering the abovementioned challenges, a reservoir-based system which can provide an effective light-triggered, controlled drug release, with minimal release in the 'off' state, would be high beneficial.

Herein, we report a photo-triggerable, hydrogel–nanoparticle hybrid scaffold that provides a chemically-defined, remotely-triggered and on-demand release of small molecule drugs (Fig. 1). Our hybrid drug delivery platform consists of three main components: (1) a photo-triggerable chemical compound, which releases a covalently-bound drug upon photo-irradiation, (2) a silica nanoparticle, which serves to covalently bind the photo-triggerable chemical compound, and (3) a poly(ethylene glycol) (PEG)-based hydrogel matrix, which serves to retain the drug-conjugated nanoparticle. Upon exposure to UV light, the activation of the photo-triggerable chemical compound is designed to initiate a series of intramolecular chemical rearrangements, which would cleave the covalently-bound drug from the nanoparticle surface and ultimately release it from the hydrogel. In this way, our hybrid scaffold combines the unique intrinsic properties of synthetic chemical compounds, three-dimensional hydrogel scaffolds and multifunctional nanoparticles in a single, reservoir-based drug delivery platform. In the current work, we demonstrate the utility of our platform to deliver a specific model drug (camptothecin) to a malignant brain tumor cell line. However, each of the comprising components of our hybrid scaffold (*i.e.* the small molecule drug, the stimuli-responsive trigger, the nanoparticle and the hydrogel) can be easily replaced to tune our platform for practically any biological application of interest, thus offering immense potential for advancing drug delivery systems.

Results and discussion

Synthesis of the photo-triggerable chemical adaptor system

A key aspect of our system relies on establishing a stable chemical linkage to attach small molecule drugs to the nanoparticle surface, while also permitting spontaneous release upon photo-irradiation (Fig. 1). This requires a synthetic approach wherein the different functionalities can be linked together and then fragmented into the individual building blocks in a controlled manner. Chemical adaptor systems (CAS) are a unique class of synthetic molecules which have been designed specifically for this purpose.[17,18] These unique molecules are based on a core molecule ('chemical adaptor') which provides a chemical linkage between multiple functional moieties (*e.g.* stimuli-responsive trigger, small molecule drug, *etc.*) that can be triggered for rapid disassembly under pre-defined conditions. In this study, we designed a photo-
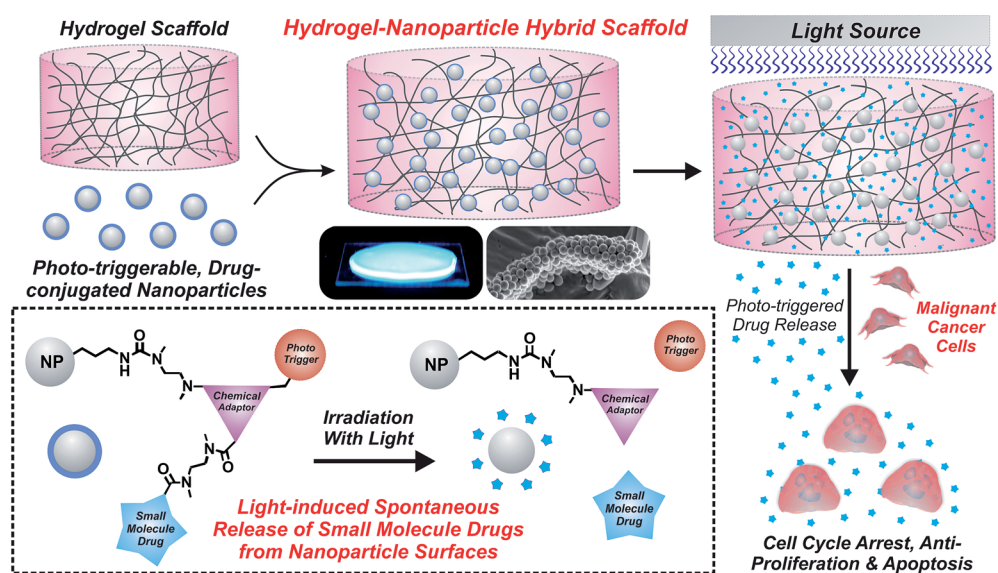

Fig. 1 Schematic illustration depicting the fabrication and application of hydrogel–nanoparticle hybrid scaffolds. Photo-triggerable, drug-conjugated silica nanoparticles were encapsulated within a PEG-based hydrogel. The subsequent photo-irradiation of the hybrid scaffold initiates a series of chemical rearrangements which ultimately releases the covalently-bound drug to induce cancer cell death.

triggerable CAS for the release of the covalently-bound model drug camptothecin (CPT), a DNA topoisomerase I inhibitor,[19] upon exposure to UV light. We utilized the commercially available 4-hydroxymandelic acid as the core chemical adaptor, which has three functional end groups available for conjugation: the benzylic hydroxyl group, the phenolic hydroxyl group and the carboxylic acid (Fig. 2). In this case, we used the benzylic hydroxyl group to link the drug molecule, the phenolic hydroxyl group to attach the photo-reactive trigger molecule and the carboxylic acid to mediate the conjugation to the nanoparticle.

The photo-triggerable CAS was synthesized step-by-step starting with 4-hydroxymandelic acid (1) as shown in Fig. 2. Briefly, 4-hydroxymandelic acid (1) was coupled with monop-rotected boc-dimethylethylenediamine in the presence of EDC and HOBt to yield compound (2). Selective alkylation of the phenolic hydroxyl group with the photo-trigger group (4,5-dimethoxy-2-nitrobenzyl bromide) resulted in the formation of an ether linkage (3). The acylation of the benzylic hydroxyl group was carried out with 4-nitrophenyl chloroformate in the presence of 4-dimethylaminopyridine and triethylamine at 0 °C to obtain the p-nitrophenyl ester (4). Finally, compound (4) was reacted with dimethylethylenediamine-conjugated CPT drug (5) using triethylamine to yield the CAS–CPT compound (6). Detailed synthetic procedures and characterization are provided in the ESI Section 1.†

Prior to attaching the CAS–CPT to the nanoparticle surface, we determined whether the CPT drug could be released upon photo-irradiation. As per the CAS–CPT design, exposure to UV light (365 nm) would trigger the cleavage of the photo-trigger group and generate an unstable phenol, which would then undergo a spontaneous rearrangement to release carbon dioxide via decarboxylation, a dimethyl urea via cyclization and the active CPT drug (see ESI Section 2† for detailed mechanistic scheme). The reaction was carefully monitored before and after photo-irradiation using mass spectroscopy, which confirmed the efficient release of CPT from the CAS molecule (see ESI Section 2† for full characterization). The HPLC assay further confirmed the release of the covalently-bound CPT molecule upon exposure to UV light, with complete release observed within 24 h (Fig. S1†). Moreover, in the absence of UV light, the CAS–CPT was observed to remain intact with no release of CPT even after 30 days of incubation, further confirming the chemical stability and light-specific sensitivity of this compound (Fig. S2†).

Conjugation of the CAS–CPT to nanoparticles

After confirming the effectiveness of the CAS in releasing the CPT drug, we proceeded to covalently attach the CAS–CPT to a nanoparticle surface. We utilized silica nanoparticles (silica NPs) to anchor the CAS–CPT since they are highly inert and stable, exhibit excellent biocompatibility and allow for facile surface functionalization.[20] Briefly, amine-terminated silica NPs (300 nm; Corpuscular, Inc) were first activated with N,N'-disuccinimidyl carbonate in the presence of N,N-diisopropylethylamine, followed by reaction with the boc-deprotected CAS–CPT to obtain the NP–CAS–CPT (Fig. 3a).

The release kinetics of the CPT drug from the photo-triggerable, drug-conjugated NPs was then examined upon photo-irradiation. The NP–CAS–CPT was dispersed in PBS and exposed to 365 nm light (2.5 mW cm^{-2}). Prior to each measurement, the nanoparticles were centrifuged and the supernatant was collected to measure the emission spectra of the free CPT (λ_{ex} = 368 nm). After photo-irradiation, a steady increase in the fluorescence intensity at 426 nm (λ_{em} of CPT) was observed (Fig. 3b). The drug release was adjusted by altering the exposure time to UV light between 0 to 20 min. Measurements acquired at 24 h demonstrate an exposure time-dependent release of CPT from the NP–CAS–CPT construct, wherein 10 min of photo-irradiation was observed to be sufficient to obtain complete drug release (Fig. 3c). The drug loading from these measurements was determined to be ~2.13 μmol CPT per gram of NP. The NP–CAS–CPT was further observed to be stable in the absence of UV exposure, with a negligible change in the spectra even after 21 days of incubation in PBS at 37° (Fig. 3d). Photo-irradiation after 21 days of incubation resulted in the
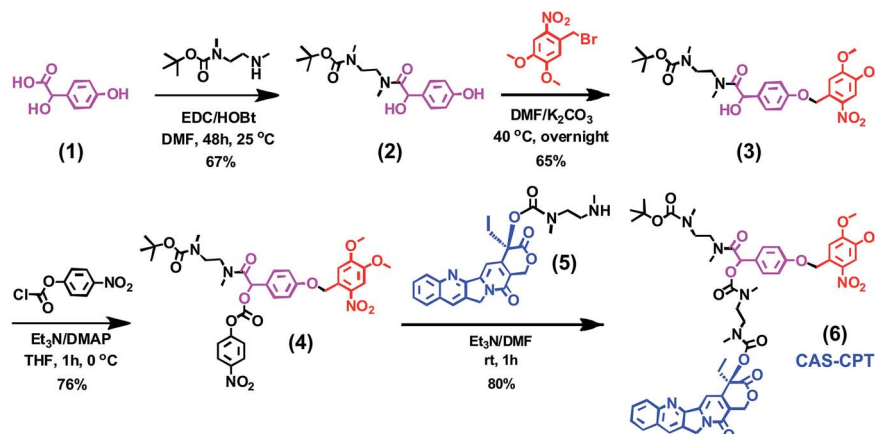

Fig. 2 Synthesis of the chemical adaptor system (CAS) bound with camptothecin (CPT). The core of the CAS (4-hydroxymandelic acid) was covalently attached with the photo-trigger group (4,5-dimethoxy-2-nitrobenzyl) and the anticancer drug (CPT).
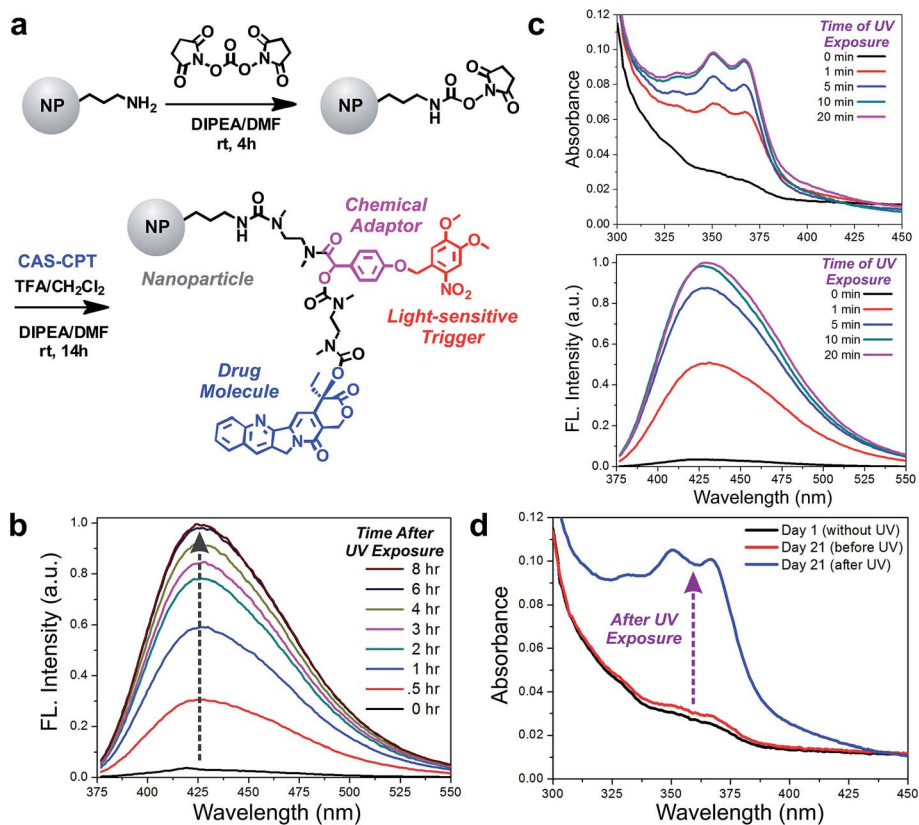
Fig. 3 The CAS–CPT conjugated nanoparticle constructs show excellent stability and photo-triggered release. (a) Scheme for conjugation of CAS–CPT on silica NPs. (b) Release of CPT monitored over time after 10 min of UV light exposure (365 nm, 2.5 mW cm^{-2}) using fluorescence spectroscopy. (c) Release of CPT measured after varying times of UV light exposure (0–20 min). Measurements were acquired 24 h after UV exposure, using absorption spectroscopy (top) and fluorescence spectroscopy (bottom, λ_{ex} = 368 nm). (d) Absorbance spectra measured over 21 days in the absence of UV exposure (black & red), followed by 10 min UV irradiation after 21 days (blue).

same level of CPT release observed earlier, indicating that the CAS–CPT complex was still intact and fully functional (Fig. 3d). This data suggests that the NP–CAS construct can serve as a reliable platform to facilitate the photo-triggered release of small molecule drugs.

Nanoparticle encapsulation within the hydrogel matrix

After demonstrating the controlled photo-induced release from the NP–CAS construct, we aimed to create a reservoir-based drug delivery system by encapsulating the drug-conjugated nanoparticles within a polymeric hydrogel matrix. Polymeric hydrogels have emerged as a popular class of materials for biological applications due to a number of attractive features, including the close resemblance to native human tissue, high water content, ease in modification of its physical and chemical properties, and the facile transport of nutrients and biomolecules.[21] While hydrogels composed of both natural and synthetic polymers have been established, poly(ethylene glycol) (PEG)-based hydrogels have been commonly used since they are biocompatible, exhibit negligible immunogenicity, prevent non-specific adhesion and are FDA-approved for various clinical applications.[22] We generated covalently cross-linked PEG hydrogels using the regioselective and highly efficient Click

chemistry reaction. In particular, Click-based hydrogel networks have been found to produce controlled architecture and have improved mechanical properties due to the controlled nature of the Click coupling reaction between orthogonal functional groups.[23,24]

We exploited these features to form our hydrogel-based reservoir by the copper(I)-catalyzed cycloaddition of azide-terminated and alkyne-terminated PEG monomers in the presence of our NP–CAS–CPT constructs (Fig. 4a). We mixed one equivalent of four-arm PEG azide (10 kDa) with two equivalents of PEG dialkyne (4 kDa) under aqueous conditions at 37 °C in the presence of sodium ascorbate (1 eq.) and copper sulfate (0.4 eq.). The NP–CAS–CPT constructs were embedded within the hydrogel by simply mixing the nanoparticles from an aqueous stock solution into the prepolymer solution prior to adding the copper catalyst. Under these conditions, the hybrid scaffolds were seen to form within 30 min. The hydrogel–NP scaffolds were washed with aqueous ethylenediamine tetraacetic acid (EDTA, 0.1 M) to remove traces of the copper, and then incubated in PBS for at least one day to allow for equilibration.

The incorporation of the NPs within the hydrogel matrix was first visualized by using pyrene dye-conjugated NPs, which show strong blue fluorescence under UV irradiation. In addition to the blue intensity observed throughout the hydrogel,

7688 | J. Mater. Chem. B, 2014, 2, 7685–7693

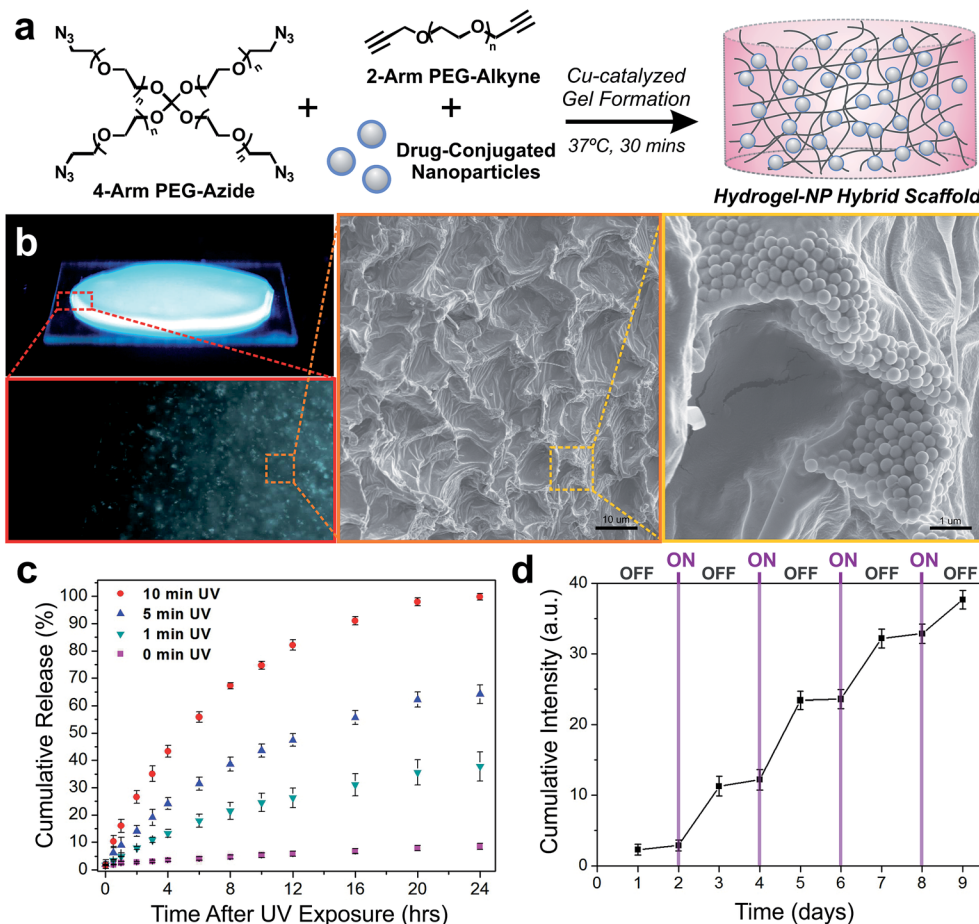This journal is © The Royal Society of Chemistry 2014

Fig. 4 Hydrogel–NP hybrid scaffolds enable the controlled and on-demand release of drugs. (a) Scheme for encapsulation of drug-conjugated NPs within PEG-based hydrogels formed using copper-catalyzed Click chemistry. (b) Fluorescence and SEM images of NPs distributed throughout the hydrogel matrix. (c) The cumulative release of CPT from hydrogel–NP hybrid scaffolds ($n = 3$) after varying times of UV light exposure (365 nm, 2.5 mW cm^{-2}), measured over 24 h after photo-irradiation. (d) Cumulative CPT release from the hydrogel–NP hybrid scaffolds ($n = 3$) with cycles of OFF (48 h) and ON (30 seconds UV light).

fluorescence microscopy provides further evidence for the uniform distribution of the NPs in the hydrogel matrix (Fig. 4b). Scanning electron microscopy (SEM) was then used to examine the fine microscopic structure of the hydrogel and the distribution of the embedded NP–CAS–CPT constructs. SEM micrographs indicate that an isotropic gel has formed which has the classic, uniform morphology reported for such hydrogels, along with an even distribution of the NPs throughout the hydrogel matrix (Fig. 4b). Additionally, the hydrogels do not show significant changes in the elastic properties upon adding increasing amounts of the NP constructs, suggesting that the underlying polymer network formed after gelation is stable and remains intact (Fig. S3†). This feature is particularly advantageous from both a drug delivery and clinical standpoint, since it can allow for the versatile loading of the drug-conjugated NP constructs without altering the mechanical properties of the hybrid scaffold.

Controlled drug release from hydrogel–NP hybrid scaffolds

The release kinetics of CPT from the hydrogel–NP hybrid scaffolds was next analyzed upon photo-irradiation. A steady increase in the fluorescence intensity ($\lambda_{em} = 426$ nm) was observed over time after photo-irradiation, reaching a saturation point within 24 h (Fig. S4†). By varying the time of photo-irradiation, the release kinetics of CPT from the hybrid scaffolds was modulated to achieve varying degrees of maximum drug release (Fig. 4c). For instance, we attained 25%, 60% and 100% cumulative CPT release using 1, 5 and 10 min UV exposure, respectively (Fig. 4c). At the same time, negligible CPT release was observed in the absence of UV exposure. In addition to achieving a predefined percentage of total release, the amount of drug released with a given time of UV exposure was further controlled by adjusting the initial NP–CAS–CPT loading within the hydrogel matrix (Fig. S5†). This type of controlled and triggered drug release, modulated simply by varying the time of photo-irradiation and the amount of NP loading within the hydrogel, can afford innumerable types of drug release profiles that can be dynamically adjusted over time.

To further demonstrate the robustness of these hydrogel–NP hybrid scaffolds, CPT release was monitored using an alternating ON/OFF exposure to light. The hybrid scaffolds were first incubated for 24 h (OFF), followed by UV light exposure for 30

This journal is © The Royal Society of Chemistry 2014

J. Mater. Chem. B, 2014, 2, 7685–7693 | 7689

seconds (ON). The gels were then kept incubated for 48 h (OFF), followed by UV light exposure for 30 seconds (ON). This cycle was repeated four times, over a span of nine days, to evaluate the repeatability and triggered release capabilities of the hydrogel–NP scaffold. The cumulative release during the ON–OFF cycling shows a stepwise drug profile, in which photo-irradiation (ON) induced a steep increase in CPT release and the absence of photo-irradiation (OFF) showed minimal release (Fig. 4d). This stepwise, photo-triggered release over an extended period of time, along with the negligible release in the OFF state, highlights the effectiveness of our hydrogel–NP hybrid scaffold as a promising remotely-triggerable, reservoir-based drug delivery system.

Hydrogel–NP hybrid scaffolds for drug delivery to cancer cells

We further evaluated the efficacy of our system in a cancer cell model. We utilized permeable support cell culture inserts (TransWell®) as depicted in Fig. 5. The hybrid scaffold was made directly within the TransWell® insert, which contains a microporous membrane that would allow for the facile transport of the released drug into the underlying culture well containing the cellular monolayer (Fig. 5a). While this experimental setup allows for the facile testing of drug release, the insertion of the culture insert containing the hydrogel–NP scaffold into the culture wells containing the cancer cells further mimics an implantable reservoir-based drug delivery platform for an *in vitro* culture system (Fig. 5b). As a proof-of-concept, we utilized human U87 glioblastoma cells expressing the mutant oncogenic epidermal growth factor receptor vIII (U87-EGFRvIII),

which are derived from an extremely aggressive form of a primary brain tumor known as glioblastoma multiforme. The brain cancer cells were first seeded into cell culture well plates (3×10^4 cells per mL) and allowed to attach for one day. Hydrogel–NP scaffolds were made, as described above, in the TransWell® inserts, rinsed with EDTA (0.1 M) and incubated in PBS for one day to allow for equilibration. The hybrid scaffolds were then irradiated with 365 nm light (10 min, 2.5 mW cm^{-2}), followed by deposition of the inserts into the culture dish containing the cancer cell monolayers (Fig. 5a).

Compared to the cells in the untreated control condition, the cells in the hydrogel only and non-irradiated hybrid scaffold conditions exhibit similar cell densities and morphology, indicating negligible toxicity from the hydrogel scaffolds and negligible non-specific release of the CPT drug from the hybrid scaffold (Fig. 5c). In contrast, the condition with the photo-irradiated hybrid scaffolds shows a significantly reduced number of viable cells, which suggests the successful triggered release and delivery of the CPT drug (Fig. 5c). After four days of incubation, the MTS assay was performed to further quantify the cellular viability. A dose-dependent trend was observed in cellular viability for the photo-irradiated conditions, wherein the cells incubated with hybrid scaffolds containing greater amounts of the drug-conjugated nanoparticles showed a greater degree of cell death (Fig. 5d). At same time, there was a negligible effect on cellular viability observed for the non-irradiated scaffolds, which further affirms the lack of non-specific drug release in the absence of photo-irradiation.
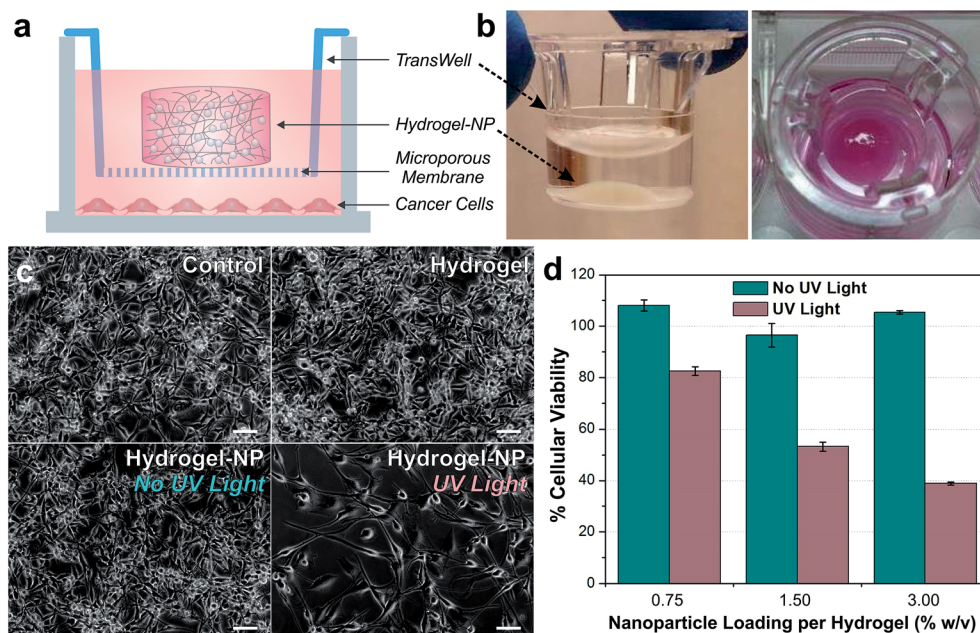

Fig. 5 Cancer cells exhibit dose-dependent sensitivity to the CPT drug photo-released from hydrogel–NP hybrid scaffolds. (a) Cell culture setup for assessing CPT drug delivery to U87 glioblastoma brain cancer cells. (b) Images of hydrogel–NP hybrid scaffolds generated in cell culture inserts. (c) Phase images of brain cancer cells after four days in varying conditions: control (untreated cells), hydrogel without NPs, hydrogel–NP without UV irradiation and hydrogel–NP with 10 min UV irradiation (365 nm, 2.5 mW cm^{-2}). Scale bars = 50 μm. (d) Cellular viability after four days in the presence of varying NP-loaded hydrogels ($n = 3$), with and without UV irradiation (normalized to control untreated cells).

7690 | *J. Mater. Chem. B*, 2014, **2**, 7685–7693

This journal is © The Royal Society of Chemistry 2014

Conclusion

Overall, we have demonstrated a unique hydrogel–nanoparticle hybrid scaffold which allowed for the remotely-triggered, controlled and on-demand release of drug molecules. Our methodology involved incorporating the distinct properties that are intrinsic to hydrogels (e.g. three-dimensional, biocompatible, in vivo tissue-mimics) and nanoparticles (e.g. large surface area-to-volume, facile surface functionalization, multifunctional) within a single hybrid platform. Such depot formulations have recently gained attention for modulating drug release.[25,26] However, compared to previous reports, we employed a robust synthetic strategy to stably link chemotherapeutic drugs to the nanoparticle surface, while simultaneously allowing for controlled drug release from the hydrogel upon photo-irradiation. The combination of these discrete components in a single hybrid system provided a number of advantages compared to conventional approaches, including chemical control over drug loading and release, negligible release in the absence of photo-irradiation, ease in adjusting drug release kinetics and high stability for long-term studies. While we have established our platform using a specific model drug and cancer cell line, the versatile design of our system allows for the replacement of any of the comprising elements, including the small molecule drug (e.g. anticancer drugs, steroids, anti-inflammatories), the stimulus-responsive trigger (e.g. light, enzyme, pH), the nanoparticle (e.g. silica, magnetic and gold nanoparticles) and the hydrogel (e.g. PEG, collagen, gelatin). In this way, our hydrogel–nanoparticle platform is potentially amendable to any type of biological application that requires the controlled release of drugs or biomolecules. We envision that our hybrid biomaterial approach will be essential for the development of advanced therapies in biomedicine.

Experimental

General synthesis of CAS–CPT & hydrogel PEG monomers

All reactions were carried out under nitrogen or argon atmosphere. All light sensitive reactions were carried out in the dark. All reagents were purchased from Acros, Sigma-Aldrich, or Alfa Aesar and used without further purification. Analytical thin layer chromatography was performed on EM Reagent 0.25 mm silica gel 60 F254 plates. Visualization was accomplished with UV light and potassium permanganate stain followed by heating. Purification of reaction products was carried out by flash column chromatography using Sorbent Technologies Standard Grade silica gel (60 Å, 230–400 mesh). The ESI† outlines the detailed synthesis and characterization of the CAS–CPT compound (ESI Section 1†), CPT release from CAS–CPT (ESI Section 2†) and the hydrogel PEG monomers (ESI Section 3†).

Conjugation of CAS–CPT to silica nanoparticles

To conjugate the CAS–CPT compound to nanoparticles, amine-terminated silica nanoparticles (silica NPs; corpuscular, Inc; Cat. no. 140360-10) were first suspended in DMF (0.5 mL). The silica NPs were reacted with N,N'-disuccinimidyl carbonate (25

mg) and N,N-diisopropylethylamine (DIPEA, 25 µL) to activate the amine group. The reaction was carried out for 4 h. In order to functionalize maximal free amine groups on the silica NP surface as possible, the reaction was repeated a total of two times. Thereafter, the silica NPs were washed with DMF, resuspended in DMF (0.5 mL) and kept at room temperature. The CAS–CPT compound was then dissolved in 0.4 mL CH_2Cl_2 and cooled to 0 °C. Trifluoroacetic acid (TFA, 25 µL) was then added dropwise and the reaction was continued in the dark at 0 °C for 45 min. The TFA with CH_2Cl_2 were removed under reduced pressure and the residue was dissolved in 750 µL DMF. The above boc-deprotected compound was reacted with amine-activated silica NPs in the presence of Et_3N (0.25 mL). The reaction was continued in the dark at room temperature overnight. The NP–CAS–CPT was purified by washing several times with DMF, followed by MeOH and finally, the product was isolated and dried.

Characterization of CPT release from NP–CAS–CPT

The solid NP–CAS–CPT powder was suspended in phosphate buffer saline (1× PBS, pH 7.4). The samples were exposed to UV light (365 nm, 2.5 mW cm^{-2}) for different times intervals (0–20 min), followed by incubation at 37 °C. Prior to each measurement, the samples were centrifuged (6000 rpm) and the CPT release was monitored from the supernatant solution using absorbance and fluorescence spectroscopy.

Preparation of nanoparticle-encapsulated hydrogels by copper-catalyzed click chemistry

The PEG monomers were prepared as described in ESI Section 3.† To form the hydrogel, PEG-tetraazide (MW = 10 kD) was reacted with two equivalents of PEG-dialkyne (MW = 4 kDa) at 37 °C under aqueous conditions in the presence of copper sulfate and sodium ascorbate as a reducing agent. Based on previously reported conditions,[24] a prepolymer solution containing a [dialkyne] : [tetraazide] : [copper] : [ascorbate] ratio of 2 : 1 : 0.4 : 1 was made. To encapsulate the drug-conjugated nanoparticles (NP–CAS–CPT) within the hydrogel matrix, the dried nanoparticle powder was dispersed in DI water to make a stock solution from which a given volume was transferred directly into the prepolymer solution. Varying amounts of NP–CAS–CPT were dispersed within the hydrogel matrix (0–3.75% w/v). After thorough vortexing and mixing, gelation was observed to occur within 30 min at 37 °C. The gels were then washed with Versene (Gibco®; 0.48 mM EDTA) to remove traces of copper and then washed extensively with 1× PBS.

Characterization of CPT release from hybrid scaffolds using fluorescence spectroscopy

The hydrogel–nanoparticle hybrid scaffolds were immersed in 1× PBS (pH 7.4) and exposed to UV light (365 nm, 2.5 mW cm^{-2}) for different time intervals (1, 5 and 10 min). The hybrid scaffolds were then incubated at 37 °C, and CPT release was monitored using fluorescence spectroscopy (λ_{ex} = 368 nm, λ_{em} = 426 nm). For control, similar conditions were carried out without exposure to UV light.

SEM preparation

The hydrogel samples were equilibrated in 1× PBS at room temperature and subsequently frozen at −80 °C for 1 h. The samples were then freeze-dried overnight, and the fractured cross-sections were mounted on aluminum studs. After sputter-coating with gold, the Zeiss Sigma field emission scanning electron microscope (FE-SEM) was used to image the samples.

Mechanical testing using rheology

Rheology experiments were performed to measure the elastic modulus (G') and viscous modulus (G'') of the gel samples. Gels were first prepared as described above and equilibrated in 1× PBS for at least one day. The Malvern Kinexus rheometer with a parallel-plate geometry was used, with a parallel plate diameter of 8 mm and gap distance of about 0.45 mm. An amplitude sweep was first carried out to identify the linear viscoelastic range of the hydrogel scaffolds. A frequency sweep was then performed with a shear strain rate of 0.1% to determine the elastic and viscous modulus for the hydrogel–nanoparticle scaffolds. All gels were elastic ($G' \gg G''$), and the elastic moduli was independent of frequency for the range examined. The elastic moduli for hydrogels containing varying NP–CAS–CPT loadings are reported at a frequency of 1 Hz.

Cell culture

U87-EGFRvIII cells were cultured in the following growth medium: DMEM (Dulbecco's modified Eagle's medium) with high glucose (Invitrogen), 10% fetal bovine serum (FBS), 1% streptomycin–penicillin, 1% glutamax (Invitrogen), hygromycin B (30 μg mL^{-1}). Cells were cultured in 12-well plates at 3×10^4 cells per mL and allowed to attach for one day.

Preparation of hybrid scaffolds in cell culture inserts

The drug release cellular studies were conducted in 12-well plates, using Transwell® cell culture inserts (1.2 cm diameter inserts, 0.4 μm pore size) to contain the hydrogel–nanoparticle hybrid scaffold. The hydrogel–nanoparticle precursor solution was prepared (see above section 2.4) under sterile conditions, deposited in the center of the Transwell® insert and kept in the 37 °C incubator for 30 min. The gels were then washed with Versene (Gibco®; 0.48 mM EDTA) for 1 h to remove traces of copper, and then washed extensively with 1× PBS. The PBS was then replaced with the cell growth media and the gel-containing inserts were irradiated with UV light (365 nm, 2.5 mW cm^{-2}, 10 min). After irradiation, the inserts (containing the hybrid scaffolds) were placed into the wells containing the cultured cells.

Cell viability assay

Cell viability was determined after four days of culture using the MTS Assay (Promega). All experiments were conducted in triplicates and the percentage of viable cells was determined following standard protocols described by the manufacturer. The data is represented as formazan absorbance at 490 nm, and normalized to the control (untreated) cells.

References

1 C. J. Kearney and D. J. Mooney, *Nat. Mater.*, 2013, **12**, 1004–1017.

2 A. Chan, R. P. Orme, R. A. Fricker and P. Roach, *Adv. Drug Delivery Rev.*, 2013, **65**, 497–514.

3 C. L. Stevenson, J. T. Santini Jr and R. Langer, *Adv. Drug Delivery Rev.*, 2012, **64**, 1590–1602.

4 B. P. Timko, T. Dvir and D. S. Kohane, *Adv. Mater.*, 2010, **22**, 4925–4943.

5 R. Farra, N. F. Sheppard Jr, L. McCabe, R. M. Neer, J. M. Anderson, J. T. Santini Jr, M. J. Cima and R. Langer, *Sci. Transl. Med.*, 2012, **4**, 122ra121.

6 B. P. Timko, M. Arruebo, S. A. Shankarappa, J. B. McAlvin, O. S. Okonkwo, B. Mizrahi, C. F. Stefanescu, L. Gomez, J. Zhu, A. Zhu, J. Santamaria, R. Langer and D. S. Kohane, *Proc. Natl. Acad. Sci. U. S. A.*, 2014, **111**, 1349–1354.

7 K. C. Hribar, M. H. Lee, D. Lee and J. A. Burdick, *ACS Nano*, 2011, **5**, 2948–2956.

8 T. Hoare, B. P. Timko, J. Santamaria, G. F. Goya, S. Irusta, S. Lau, C. F. Stefanescu, D. Lin, R. Langer and D. S. Kohane, *Nano Lett.*, 2011, **11**, 1395–1400.

9 C. S. Kumar and F. Mohammad, *Adv. Drug Delivery Rev.*, 2011, **63**, 789–808.

10 F. Ercole, T. P. Davis and R. A. Evans, *Polym. Chem.*, 2010, **1**, 37–54.

11 C. Alvarez-Lorenzo, L. Bromberg and A. Concheiro, *Photochem. Photobiol.*, 2009, **85**, 848–860.

12 G. Liu, W. Liu and C.-M. Dong, *Polym. Chem.*, 2013, **4**, 3431–3443.

13 B. Yan, J. C. Boyer, D. Habault, N. R. Branda and Y. Zhao, *J. Am. Chem. Soc.*, 2012, **134**, 16558–16561.

14 N. Fomina, C. McFearin, M. Sermsakdi, O. Edigin and A. Almutairi, *J. Am. Chem. Soc.*, 2010, **132**, 9540–9542.

15 H.-M. Lee, D. R. Larson and D. S. Lawrence, *ACS Chem. Biol.*, 2009, **4**, 409–427.

16 I. Tomatsu, K. Peng and A. Kros, *Adv. Drug Delivery Rev.*, 2011, **63**, 1257–1266.

17 A. Gopin, C. Rader and D. Shabat, *Bioorg. Med. Chem.*, 2004, **12**, 1853–1858.

18 A. Gopin, N. Pessah, M. Shamis, C. Rader and D. Shabat, *Angew. Chem., Int. Ed.*, 2003, **42**, 327–332.

19 L. F. Liu, S. D. Desai, T. K. Li, Y. Mao, M. Sun and S. P. Sim, *Ann. N. Y. Acad. Sci.*, 2000, **922**, 1–10.

7692 | *J. Mater. Chem. B*, 2014, **2**, 7685–7693

This journal is © The Royal Society of Chemistry 2014

20 M. L. Foglia, G. S. Alvarez, P. N. Catalano, A. M. Mebert, L. E. Diaz, T. Coradin and M. F. Desimone, *Recent Pat. Biotechnol.*, 2011, **5**, 54–61.

21 T. R. Hoare and D. S. Kohane, *Polymer*, 2008, **49**, 1993–2007.

22 C.-C. Lin and K. Anseth, *Pharm. Res.*, 2009, **26**, 631–643.

23 C. A. DeForest and K. S. Anseth, *Nat. Chem.*, 2011, **3**, 925–931.

24 M. Malkoch, R. Vestberg, N. Gupta, L. Mespouille, P. Dubois, A. F. Mason, J. L. Hedrick, Q. Liao, C. W. Frank, K. Kingsbury and C. J. Hawker, *Chem. Commun.*, 2006, 2774–2776.

25 L. E. Strong, S. N. Dahotre and J. L. West, *J. Controlled Release*, 2014, **178**, 63–68.

26 D. L. Sellers, T. H. Kim, C. W. Mount, S. H. Pun and P. J. Horner, *Biomaterials*, 2014, **35**, 8895–8902.